JACS
JOURNAL OF THE AMERICAN CHEMICAL SOCIETY
Article
pubs.acs.org/JACS

Formation and Characterization of a Molecule–Metal–Molecule Bridge in Real Space

Florian Albrecht,* Mathias Neu, Christina Quest, Ingmar Swart,‡ and Jascha Repp

Institute of Experimental and Applied Physics, University of Regensburg, 93053 Regensburg, Germany

Supporting Information

ABSTRACT: Metal–organic complexes were formed by means of inelastic excitations in a scanning tunneling microscope (STM). The electronic structure of the complex was characterized using STM imaging and spectroscopy. By exploiting the symmetry of the complex, its electronic structure can be rationalized from linear combinations of molecular orbitals. The actual bonding geometry, which cannot be inferred from STM alone, was determined from atomic force microscopy images with atomic resolution. Our study demonstrates that the combination of these techniques enables a direct quantification of the interplay of geometry and electronic coupling in metal–organic complexes in real space.

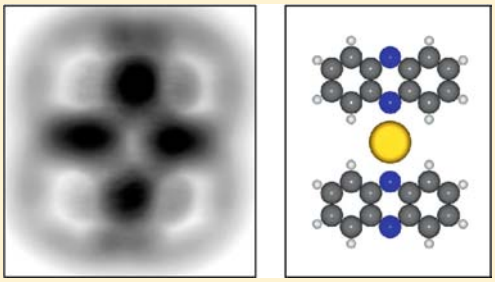

INTRODUCTION

Whereas most chemical reactions are studied in solution, in the gas phase, or at their interfaces, some applications demand the development of dry, on-surface chemistry. For example, if molecular electronics in the future is to comprise any circuitry, molecules with a delocalized electronic π-system need to be electronically coupled together. Whereas on metal surfaces quite a few examples for such a coupling exist,[1−7] a useful molecular electronic device would require being built up on the surface of an insulator.[8,9]

The tremendous progress in recent years in the development of various scanning-probe-based techniques offers the prospect of obtaining a complete quantum chemical picture of such dry, on-surface chemical reactions when combined in a single experiment. Single-molecule chemistry[1,10−12] by means of scanning-probe microscopy enables characterization of chemical bonding in real space and in an atomically well-defined environment. The use of ultrathin insulating films in such experiments made it possible to decouple molecular structures from a conductive support and thereby enable the visualization of the frontier orbitals of constituents and product.[13−15] Recently, noncontact atomic force microscopy (nc-AFM) has been used to resolve the chemical structure of molecules.[14,16−18] The combination of these techniques offers the prospect of unraveling chemical reaction mechanisms on surfaces, thereby providing an understanding of the interplay between geometry and electronic coupling in metal–organic complexes.

Here, we present a combined scanning tunneling microscopy (STM)/AFM study of complex formation between phenazine molecules and individual gold atoms deposited on an ultrathin insulating film. Using atomically resolved AFM images, we directly identify between which atoms chemical bonding has occurred. The electronic structure of the reactants and complex is characterized using scanning tunneling spectroscopy (STS). This technique is used to probe the energetic position as well as the nodal plane structure of the frontier orbitals of the reactants and of the complex. By exploiting the symmetry of the complex, its electronic structure can be rationalized from linear combinations of molecular orbitals; i.e., our results provide a direct experimental observation of this basic quantum chemical principle. Accompanying density functional theory (DFT) calculations support the applicability of this basic model. The observed peak spacing in STS data provides a measure of the electronic coupling strength.

EXPERIMENTAL SECTION

The experiments were carried out with two microscopes, a modified commercial (SPS-CreaTec) STM and a home-built combined STM/AFM, both operated in ultrahigh vacuum at a temperature of 5 K. The AFM, based on the qPlus tuning fork design,[19] was operated in the frequency modulation mode.[20] Sub-angstrom oscillation amplitudes have been used to maximize the lateral resolution.[21] The bias voltages refer to the sample with respect to the tip. The Cu(111) single-crystal samples were cleaned by several sputtering and annealing cycles. NaCl was evaporated thermally, while the sample temperature was kept between 280 and 315 K, so that defect-free, (100)-terminated NaCl islands were formed.[22,23] All experiments were carried out on a bilayer of NaCl on Cu(111). A small amount of CO was dosed onto the surface for tip functionalization during AFM experiments.[16] Individual phenazine molecules and gold atoms were evaporated onto the sample at $T \cong 5$ K, with the sample located in the microscope. DFT calculations of the free phenazine monomer and the complex were performed using the ADF 2012 program package.[24,25]

RESULTS AND DISCUSSION

Figure 1a,b shows the synthesis of the complex from two individual phenazine molecules and an Au atom induced by means of STM manipulation.[11,13−15,27] Prior to the reaction,

Received: April 24, 2013
Published: June 7, 2013

   dx.doi.org/10.1021/ja404084p | J. Am. Chem. Soc. 2013, 135, 9200−9203

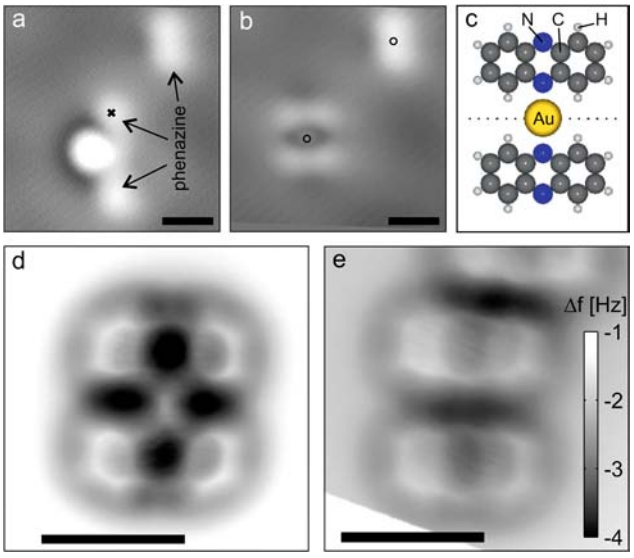

Figure 1. Complex formation and analysis of bond structure. (a) Prior to the complex formation, two phenazine molecules are adsorbed close to a gold anion. To initiate bond formation, the tip was positioned at the location indicated by the cross, and the bias voltage was ramped down to −2.5 V. (b) In a single step, a symmetric phenazine−gold−phenazine complex has formed (for (a) and (b), I = 1.0 pA, V = 0.05 V). (c) Sphere model of the phenazine−gold−phenazine complex in the geometry as deduced from AFM imaging. Carbon, nitrogen, hydrogen, and gold atoms are represented as indicated in the model. (d) Constant-height Δf image of a phenazine−gold−phenazine complex. The only bonds that formed are between the gold atom and the adjacent aromatic nitrogen atoms (A = 0.35 Å, V = 0 V, Δz = +0.1 Å).[26] (e) Constant-height Δf image of two nonbonded phenazine molecules, for comparison (A = 0.5 Å, V = 0 V, Δz = +0.3 Å).[26] All scale bars refer to 10 Å.

two phenazine molecules are adsorbed close to a negatively charged gold atom (Figure 1a). The synthesis was induced by positioning the tip above one of the molecules (cf. cross in Figure 1a) and ramping down the bias voltage to −2.5 V. A subsequently taken STM image reveals that a symmetric phenazine−gold−phenazine structure has formed, as is displayed in Figure 1b. Identical structures have been formed eight times. In the example shown here, the structure formed in a single excitation step, whereas on other occasions an intermediate step, in which only one phenazine seemed to be bonded to the gold atom, was also observed.

Although the bond motif was chosen such that a bond between the metal atom and the aromatic nitrogen in the molecules was expected, carbon−carbon bonds may have been formed in this reaction.[5,28] To unambiguously identify which atoms are involved in bond formation, AFM constant-height Δf images were acquired at small oscillation amplitudes with CO-terminated tips as proposed by Gross et al.[16] Figure 1d shows such an image of the phenazine−gold−phenazine complex. It clearly reveals that bonds have formed between the metal atom and the aromatic nitrogen atoms. No additional C−C bonds are observed. For comparison, Figure 1e shows a constant-height Δf image of two nonbonded phenazine molecules that are as close to each other as the ones in the complex. The geometry of the complex as deduced from AFM imaging is shown in Figure 1c. Complex formation was found to be reversible. After breaking one of the N−Au bonds, the separated phenazine molecule showed identical features in STM images as prior to the complex formation.

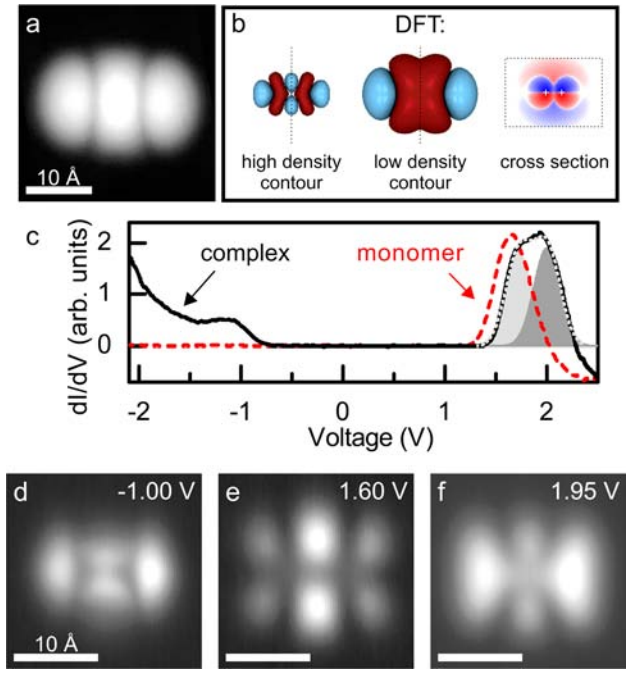

Figure 2. Differential conductance spectroscopy and dI/dV maps of an individual phenazine molecule and a phenazine−gold−phenazine complex. (a) STM constant-current image of the LUMO of an individual phenazine molecule (I = 2.5 pA, V = 1.65 V). (b) Contour of the DFT-calculated phenazine LUMO at high and low orbital density. The shape of the latter agrees well with the STM image in (a). Low- and high-density contours show different signs of the orbital structure at the center. The sign change can also be seen in the corresponding orbital density cross section (along dashed lines) through the center of the molecule. White crosses indicate the positions of the nitrogen atoms. The density scale is logarithmic. (c) Differential conductance (dI/dV) spectra of a phenazine monomer (dashed red curve) and a phenazine−gold−phenazine complex (solid black curve). Spectra were acquired at the center of monomer and complex as indicated by black circles in Figure 1b. In the experimentally accessible region, the phenazine monomer exhibits only one resonance centered at 1.7 V. In contrast, the complex shows one peak at negative bias and two close-lying peaks at positive bias voltage. Gray and light gray filled areas indicate two Gaussians that result in a good fit of the spectrum at positive bias (the dotted gray line shows the sum of the two Gaussians). Data points are averaged over 28 mV. (d−f) Constant-height dI/dV maps of a complex acquired at the indicated bias voltages. The complex is oriented as depicted in Figure 1c.

The electronic structure of individual phenazine molecules, as well as that of the complex, were studied using differential conductance (dI/dV) spectra and maps (Figure 2). The spectrum of the monomer exhibits a single peak centered at 1.7 V corresponding to the negative ion resonance. The constant current image acquired at the peak position shows a three lobe structure corresponding to the lowest unoccupied molecular orbital (LUMO) density, as can be seen in comparison to Figure 2b. Note that the molecular orbital is probed at a very low density in our STM experiments.[29]

In contrast, the complex exhibits several features in the dI/dV spectrum, one peak at negative bias,[30] and a trapezoidal-shaped feature at positive bias. The shape of the latter suggests that it consists of two close-lying peaks. The corresponding dI/dV maps show three different orbitals, confirming that there are indeed two close-lying peaks at positive bias in the dI/dV

dx.doi.org/10.1021/ja404084p | J. Am. Chem. Soc. 2013, 135, 9200−9203

spectrum belonging to different molecular orbitals. The fact that the differential conductance spectra of the complex and individual phenazine molecules are qualitatively different directly establishes that chemical bonding has occurred,[15] in agreement with the AFM images.

At this point it needs to be emphasized that the dI/dV map of the highest occupied molecular orbital (HOMO) of the complex at negative bias shows a depression at the position of the gold atom (see Figure 2d). As the HOMO is usually assumed to be a bonding orbital, this observation at first glance suggests that no bonding takes place at the gold atom. This highlights the importance of the complementary characterization by means of atomically resolved AFM. This apparent contradiction will be resolved further below.

The charge state of individual phenazine molecules was identified by their effect on the interface state scattering.[31−33] Individual phenazine molecules do not scatter the surface state electrons; hence, they are neutral. Note that gold atoms are known to have two stable charge states on this surface.[31] The complex is found to scatter the interface state electrons, indicating that it is negatively charged. A negatively charged complex has an even number of electrons, which is in line with the observation of different orbital structures at positive and negative bias voltage polarity.[13] It is also consistent with the lower apparent height of the phenazine part of the complex as compared to individual phenazine molecules in low bias STM images (see Figure 1a,b).[33]

Next, we turn to the discussion of the orbital structure of the complex. When comparing the nodal plane structure of the dI/dV maps of the individual phenazine molecules with that of the complex, one realizes that all three orbitals of the complex (Figure 2d−f) show nodal planes at the positions where two close-lying nonbonded phenazine molecules would also have nodal planes. The only differences lie in the nodal plane structure along the symmetry plane separating the two phenazine constituents (cf. dotted line in Figure 1c). Hence, all orbitals appear to be composed of the LUMOs of the individual phenazine molecules but with varying phases. As discussed above, only one state (LUMO) is observed in the differential conductance spectrum of an individual phenazine molecule. DFT calculations showed that the LUMO is not degenerate and separated by 4 and 1.8 eV from the HOMO and the LUMO+1, respectively.[25] For the gold atoms, also only one state is expected to be close to the Fermi level, namely the 6s state.[31]

We will now apply a basic quantum chemical model to rationalize the electronic structure of the complex: the linear combination of orbitals method.[34−37] To apply the model, we combine the two phenazine LUMOs and the Au 6s state while making use of the above-mentioned symmetry plane to form three complex orbitals. All orbitals of the complex must be either symmetric or antisymmetric with respect to the corresponding mirror operation. The two LUMOs of the two phenazine molecules thus form a symmetric and an antisymmetric combination. The gold 6s state can only contribute to the symmetric combination of the two LUMOs because of its s-character. Since the numbers of resulting orbitals must correspond to the number of linearly combined orbitals, this leaves us with one antisymmetric orbital without a contribution from the gold 6s state and two symmetric orbitals, in which the gold 6s state contributes with opposite sign. The above reasoning is sketched in Figure 3. Different colors indicate different signs of the wave function. Note the good

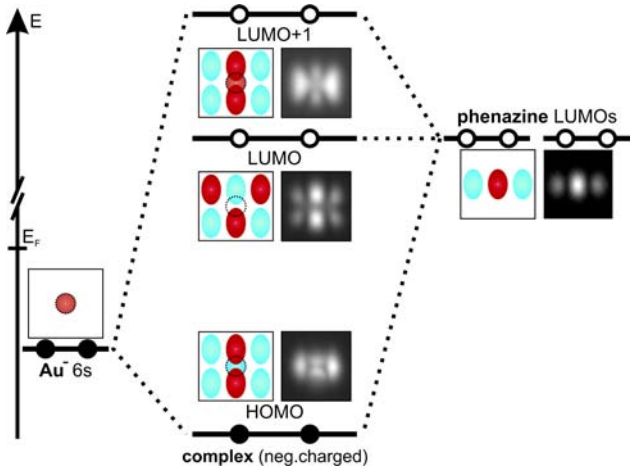

Figure 3. Schematic level diagram and basic orbital model. Light blue and dark red indicate different signs of the wave function; depicted in top view. The three constituents' orbitals being combined are the Au^- 6s state (left) and two unoccupied phenazine LUMOs (right). Due to the complex's symmetry, only the phenazine LUMOs couple to the complex's LUMO. The Au 6s contributes to the complex's HOMO and LUMO+1.[25]

agreement of the nodal plane structure predicted by this basic quantum chemical model and the experimental dI/dV images. DFT-calculated orbital images of the complex are shown in the Supporting Information.[25]

Key to understanding the shape of the HOMO is the realization that the phenazine LUMOs have a nodal plane in the molecule plane. If the gold atom is closer to the surface than the two phenazine molecules, it couples to the lower part of the wave function that has opposite sign from its value probed by the STM tip from above. Hence, for an in-phase coupling below the molecular plane, the STM senses two nodal planes from the top giving rise to the depression in the HOMO image at the position of the gold atom. The appearance of the LUMO+1 can be rationalized by similar arguments.

Phenazine molecules are found to be oriented along the polar direction of the NaCl film and their centers are located at Cl bridge sites. The adsorption site of the phenazine monomer does not change upon complex formation. The center to center distance of the phenazine molecules within the complex equals 2 times the spacing of polar rows in NaCl (8 Å). Details of the adsorption site determination can be found in the Supporting Information.[25]

Now we turn to the discussion of the energies of the resonances. The gold 6s state contributes one electron to the frontier orbitals of the complex. Because of the overall negative charge of the complex, there is one additional electron. Since only unoccupied non-degenerate states of the phenazine molecules contribute to the orbitals of the complex, one of the three orbitals of the complex is doubly occupied and the other two states remain empty. As the HOMO and the LUMO resonances correspond to the temporary removal and addition of an electron, respectively, their peak separation in the dI/dV spectrum is partially due to the Coulomb charging energy.[38] However, as the peaks corresponding to LUMO and LUMO+1 both involve the temporary addition of one electron to an orbital with similar spatial extension, their peak separation can be interpreted to be the energy difference between the two electronic states.[39] Fitting these peaks in the dI/dV spectrum of the complex at the positive bias side with two Gaussians of the

dx.doi.org/10.1021/ja404084p | J. Am. Chem. Soc. 2013, 135, 9200−9203

same width yields a peak spacing of 0.30 ± 0.03 eV (Figure 2c). The good agreement of the experimental LUMO and LUMO +1 images with symmetric and antisymmetric combinations of the phenazine's LUMOs will allow for a quantitative interpretation of their energy separation in analytical models. We would like to emphasize that, whereas DFT-calculated orbital images of the complex also qualitatively agree with the experimental observations,[25] the interpretation in terms of an electronic coupling is not straightforward from DFT simulations but can be provided by analytical models.

■ CONCLUSION

In summary, we described a model on-surface synthesis reaction on the single-molecule level. Using combined STM and AFM, the electronic and geometric structure of reactants and products were characterized. Both the energetic positions, as well as the nodal plane structure of the orbitals of the metal–ligand complex can be explained by the linear combination of orbitals method. Hence, our study demonstrates that the combination of STM and AFM enables a direct quantification of the interplay of geometry and electronic coupling in metal–organic complexes in real space.

■ ASSOCIATED CONTENT

Ⓢ Supporting Information

Experimental determination of the adsorption site, computational details for our DFT calculations, and calculated electronic level spacing of the monomer; calculated orbital contours, cross sections through these orbitals, and calculated electronic level spacing for different geometries and charge states for the complex. This material is available free of charge via the Internet at http://pubs.acs.org.

■ AUTHOR INFORMATION

Corresponding Author

florian.albrecht@physik.uni-regensburg.de

Present Address

‡I.S.: Debye Institute for Nanomaterials Science, Faculty of Science, Utrecht University, Utrecht, The Netherlands

Notes

The authors declare no competing financial interest.

■ ACKNOWLEDGMENTS

The authors thank N. Pavliček and F. J. Giessibl for fruitful discussions. Financial support from the Deutsche Forschungsgemeinschaft (GRK 1570, and SPP 1243) and the Volkswagen Foundation through its Lichtenberg Programm is acknowledged. I.S. is grateful for funding from the Nederlandse Organisatie voor Wetenschappelijk Onderzoek (NWO/Chemical Sciences, VENI-grant 722.011.007).

■ REFERENCES

(1) Hla, S.-W.; Bartels, L.; Meyer, G.; Rieder, K.-H. *Phys. Rev. Lett.* **2000**, *85*, 2777.

(2) Pawin, G.; Wong, K. L.; Kim, D.; Sun, D.; Bartels, L.; Hong, S.; Rahman, T. S.; Carp, R.; Marsella, M. *Angew. Chem., Int. Ed.* **2008**, *47*, 8442.

(3) Gutzler, R.; Walch, H.; Eder, G.; Kloft, S.; Heckl, W. M.; Lackinger, M. *Chem. Commun.* **2009**, 4456.

(4) Grill, L.; Dyer, M.; Lafferentz, L.; Persson, M.; Peters, M. V.; Hecht, S. *Nat. Nanotechnol.* **2007**, *2*, 687.

(5) Cai, J.; Ruffieux, P.; Jaafar, R.; Bieri, M.; Braun, T.; Blankenburg, S.; Muoth, M.; Seitsonen, A. P.; Saleh, M.; Feng, X.; Muellen, K.; Fasel, R. *Nature* **2010**, *466*, 470.

(6) Lafferentz, L.; Eberhardt, V.; Dri, C.; Africh, C.; Comelli, G.; Esch, F.; Hecht, S.; Grill, L. *Nature Chem.* **2012**, *4*, 215.

(7) DiLullo, A.; Chang, S.-H.; Baadji, N.; Clark, K.; Klöckner, J.-P.; Prosenc, M.-H.; Sanvito, S.; Wiesendanger, R.; Hoffmann, G.; Hla, S.-W. *Nano Lett.* **2012**, *12*, 3174.

(8) Maier, S.; Fendt, L.-A.; Zimmerli, L.; Glatzel, T.; Pfeiffer, O.; Diederich, F.; Meyer, E. *Small* **2008**, *4*, 1115.

(9) Kittelmann, M.; Rahe, P.; Nimmrich, M.; Hauke, C. M.; Gourdon, A.; Kühnle, A. *ACS Nano* **2011**, *5*, 8420.

(10) Lee, H. J.; Ho, W. *Science* **1999**, *286*, 1719.

(11) Hahn, J. R.; Ho, W. *Phys. Rev. Lett.* **2001**, *87*, 166102.

(12) Shiotari, A.; Kitaguchi, Y.; Okuyama, H.; Hatta, S.; Aruga, T. *Phys. Rev. Lett.* **2011**, *106*, 156104.

(13) Repp, J.; Meyer, G.; Paavilainen, S.; Olsson, F. E.; Persson, M. *Science* **2006**, *312*, 1196.

(14) Mohn, F.; Repp, J.; Gross, L.; Meyer, G.; Dyer, M. S.; Persson, M. *Phys. Rev. Lett.* **2010**, *105*, 266102.

(15) Liljeroth, P.; Swart, I.; Paavilainen, S.; Repp, J.; Meyer, G. *Nano Lett.* **2010**, *10*, 2475.

(16) Gross, L.; Mohn, F.; Moll, N.; Liljeroth, P.; Meyer, G. *Science* **2009**, *325*, 1110.

(17) Gross, L.; Mohn, F.; Moll, N.; Meyer, G.; Ebel, R.; Abdel-Mageed, W. M.; Jaspars, M. *Nature Chem.* **2010**, *2*, 821.

(18) Mohn, F.; Gross, L.; Meyer, G. *Appl. Phys. Lett.* **2011**, *99*, 053106.

(19) Giessibl, F. J. *Appl. Phys. Lett.* **2000**, *76*, 1470.

(20) Albrecht, T. R.; Grütter, P.; Horne, D.; Rugar, D. *J. Appl. Phys.* **1991**, *69*, 668.

(21) Giessibl, F. J. *Rev. Mod. Phys.* **2003**, *75*, 949.

(22) Repp, J.; Meyer, G.; Rieder, K.-H. *Phys. Rev. Lett.* **2004**, *92*, 036803.

(23) Bennewitz, R.; Barwich, V.; Bammerlin, M.; Loppacher, C.; Guggisberg, M.; Baratoff, A.; Meyer, E.; Güntherodt, H.-J. *Surf. Sci.* **1999**, *438*, 289.

(24) te Velde, G.; Bickelhaupt, F. M.; Baerends, E. J.; Guerra, C. F.; van Gisbergen, S. J. A.; Snijders, J. G.; Ziegler, T. *J. Comput. Chem.* **2001**, *22*, 931.

(25) Further information is provided as Supporting Information.

(26) The values *A*, *V*, and Δz refer to the oscillation amplitude, voltage, and change in vertical tip position with respect to the set-point of 1 pA at 0.4 V above NaCl, respectively. Positive values of Δz refer to the tip being closer to the sample.

(27) Swart, I.; Sonnleitner, T.; Niedenführ, J.; Repp, J. *Nano Lett.* **2012**, *12*, 1070.

(28) Bjork, J.; Stafstrom, S.; Hanke, F. *J. Am. Chem. Soc.* **2011**, *133*, 14884.

(29) Repp, J.; Liljeroth, P.; Meyer, G. *Nature Physics* **2010**, *6*, 975.

(30) The first feature at the negative bias side does not appear like an isolated peak since it is influenced by the peak at more negative bias values.

(31) Repp, J.; Meyer, G.; Olsson, F. E.; Persson, M. *Science* **2004**, *305*, 493.

(32) Olsson, F. E.; Paavilainen, S.; Persson, M.; Repp, J.; Meyer, G. *Phys. Rev. Lett.* **2007**, *98*, 176803.

(33) Swart, I.; Sonnleitner, T.; Repp, J. *Nano Lett.* **2011**, *11*, 1580.

(34) Lennard-Jones, J. E. *Trans. Faraday Soc.* **1929**, *25*, 668.

(35) Pauling, L. *Chem. Rev.* **1928**, *5*, 173.

(36) Atkins, P. W. *Physical Chemistry*; Oxford University Press: Oxford, UK, 1998.

(37) Mortimer, R. G. In *Physical Chemistry*; Walker, J., Ed.; Benjamin/Cummings: San Francisco, CA, 1993.

(38) Repp, J.; Meyer, G.; Stojković, S. M.; Gourdon, A.; Joachim, C. *Phys. Rev. Lett.* **2005**, *94*, 026803.

(39) Petty, M. *Molecular Electronics: From Principles to Practice*; Wiley Series in Materials for Electronic & Optoelectronic Applications; John Wiley & Sons: New York, 2007.